Indian Journal of Chemistry
Vol. 64, January 2025, pp. 43-53
DOI: 10.56042/ijc.v64i1.14056

Synthesis, spectral characterization, DFT calculations and investigation of anticancer properties of carbothioamide and metal (Fe^{II} and Cr^{III}) complexes

Elif Güney[a], Koray Sayin*[a] & Hayreddin Gezegen[b]

[a] Sivas Cumhuriyet University, Faculty of Science, Department of Chemistry 58140 Sivas, Türkiye

[b] Sivas Cumhuriyet University, Faculty of Health Science, Department of Nutrition and Dietetics 58140 Sivas, Türkiye

E-mail: krysayin@gmail.com, ksayin@cumhuriyet.edu.tr

Received 29 September 2024; accepted(revised) 27 December 2024

Schiff base and its metal complexes have a broad application in areas such as medicine, pharmacy, cosmetics, agriculture, plastic industry, dyestuff production, *etc.* Recently, the anticancer activities of these compounds have been investigated, and it is a matter of curiosity how the effectiveness changes with complexation. 2-(1-(2-Hydroxyphenyl) ethylidene) hydrazine-1-carbotioamide (HL) and its metal (Fe^{II} and Cr^{III}) complexes have been synthesized and investigated computationally and experimentally. In the calculations, B3LYP-D3/6-31+G(d) for HL and B3LYP-D3/6-31+G(d)(LANL2DZ) for metal complexes have been used. Anticancer properties of these complexes have been investigated against three different cell lines which are breast cancer (MCF-7), colorectal cancer (HT-29) and gastric cancer (SNU-16). XTT test has been used in the cell viability assays. It is found that the studied compounds are active against breast cancer and Fe(II) complex has shown the best activity. Structural properties of compound have been examined computationally and experimentally. Electronic properties of the studied compounds (for HL) have been investigated by Hirshfeld surface analyses and MEP maps. Anticancer properties of studied compounds have been investigated by cell viability assays. It is found that synthesized compounds are only active against breast cell line, MCF-7. The best compound is found as [FeL_2] due to the fact that its IC_{50} has been calculated as 1.62 μM.

Keywords: Carbotioamide, Metal complex, DFT, Hirshfeld surface analysis, Anticancer properties

Small molecules contain azomethine (–C=N–) functional group among the Schiff bases[1] and has a wide range of uses such as in medicine, pharmacy, cosmetics, agriculture, plastic industry, dyestuff production, *etc.* The importance of bases is increasing day by day. Due to its chemotherapeutic properties, it has a wide range of usage in the pharmaceutical industry. Schiff bases, which are generally colored and transparent solids, also have an important place in biochemistry and analytical chemistry. Metal ions show strong bonding properties with Schiff bases. Schiff bases attract great attention due to their field of use; especially metal complexes of Schiff bases contain sulfur. Many studies have been conducted on it due to its antitumor, antibacterial and antiviral properties. Application areas vary depending on the active groups contained in Schiff bases and complexes[2].

Schiff bases have an important role in both industrial and biological uses[3]. Some Schiff derivatives have a wide range of uses in pharmacological and biological applications[4,5]. It is known that Schiff bases containing the imine (–C = N) bond have important biological activity. In particular, the synthesized Schiff bases are required to contain nitrogen atom in order to have high biological activity. Therefore, the interest and focus of many researchers is on imine compounds that are Schiff bases[6]. Schiff bases are azomethines, which are stable and easily synthesized; In addition to being used in many applications, especially in antifungal, antibacterial, antioxidant, antitumor, anti-inflammatory and antipyretic fields, Schiff bases have a special importance in the fields of pharmacology and medicine due to their structure. Moreover, it is known that these structures exhibit anticancer properties[4,6]. This study is based on 2-(1-(2-hydroxyphenyl)ethylidene)hydrazine-1-carbotioamide (HL)[7] and two different metal complexes (ML2) shown in Fig. 1.

The compounds shown in Fig. 1 were synthesized under appropriate conditions and characterized by spectral methods. Single crystal XRD analysis of the HL compound was performed and Hirshfeld surface

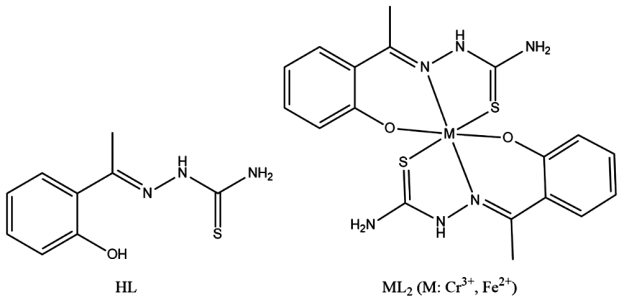

Fig. 1 — Shematic structure of HL and its metalcomplexes

analysis was performed. All experimental results were supported by computational chemistry methods. B3LYP-D3/6-31+G(d) for HL compound and B3LYP-D3/6-31+G(d)(LANL2DZ) levels for metal complexes were chosen as the calculation level. Finally, the activities of the relevant molecules against breast, stomach and colon cancer were determined by the XTT test. In this study, it was observed that the anticancer properties of Schiff bases increased with complexation. It was determined that the relevant molecules were effective against breast cancer, and the best among them was the Fe(II) complex.

Experimental Section

Materials

2′-hydroxyacetophenone, thiosemicarbazide, iron(II) chloride tetrahydrate, chromium (III) nitrate nonahydrate, ethanol (99%, HPLC grade), DMSO-D6 were purchased from commercial suppliers and used without any purification.

Measurements

Melting points were recorded in open capillary tubes by using Electrothermal IA9100. The verification of the reaction completion was done by thin layer chromatography (TLC) on Merck silica gel plates (60 F254 aluminium sheets), visualized under UV light. NMR spectra were collected using JEOL (400 MHz) JNM-ECZ400S/L1 spectrometer. IR-ATR spectra were obtained using a Bruker Tensor II FT-IR spectrophotometer. Data for X-ray crystallography for the ligand were collected at 296(2) K on a Bruker SMART APEX II diffractometer using Mo-Kα radiation (λ = 0.71073 Å). Data reduction was performed using Bruker SAINT. SHELXS97 was used to solve and SHELXL2014/6 to refine the structure[8]. Agilent Technology Inc. of 1260 Infinity HPLC System was coupled with 6530 Q-TOF LC/MS detector and ZORBAX SBC18 (2.1×50 mm, 1.8 μm) column.

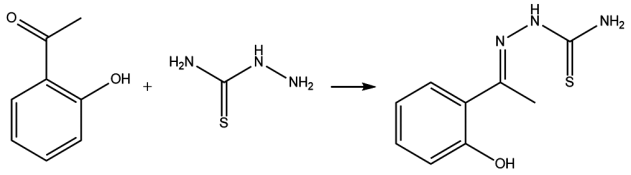

Fig. 2 — Synthesis route of the related Schiff bases

Synthetic Procedures

Synthesis of Carbotioamide Derivative

2'-hydroxyacetophenone (1 mmol) was dissolved in 20 ml of ethanol and allowed to stir. A small amount of p-toluene sulfonic acid was added to the mixture and after 5 minutes, thiosemicarbazide (1.1 mmol) was added and allowed to reflux. At the end of the reaction, which lasted 3 hours, the completion of the reaction was checked by thin layer chromatography (10:1 dichloromethane and methanol). The material was kept in the refrigerator overnight and the product was filtered through filter paper, washed with ethanol and dried. The synthesis scheme is shown in Fig. 2. The obtained crude product was purified by recrystallization in methanol. Synthesized compound was characterized by using spectral techniques which are IR-ATR, ^{1}H-NMR, ^{13}C-NMR and LC/QTOF-MS. These spectra are shown in Supporting Information Fig. S1 – S4, respectively.

2-(1-(2-Hydroxyphenyl)ethylidene)hydrazine-1-carbotioamide (HL): Yellow crystals. Yield 84%. m.p.146-149°C. IR (ATR): 3405, 3286, 3139, 2954, 1927, 1890, 1844, 1806, 1589, 1519, 1495, 1443, 1278, 1237, 1165, 1107, 1051, 821, 762, 602, 527, 501 cm^{-1}; ^{1}H NMR (400 MHz, DMSO-d_6): δ 12.69, 10.58 (2H), 8.10, 7.47 (d, J = 7.7 Hz, 1H), 7.26 – 7.11 (m, 1H), 6.81 (dd, J = 7.9, 2.9 Hz, 2H), 2.26 (3H); ^{13}C NMR (101 MHz, DMSO-d_6): δ 181.17, 157.79, 153.66, 131.11 (2C), 128.79, 119.17, 117.43, 24.67; LC/QTOF-MS: *m/z* [M-H] ($C_9H_{10}N_3OS$): Calcd 208.055. Obsd: 208.0552.

Synthesis of Cr(III) Complex

The synthesized carbotioamide compound (2 mmol) was heated in 20 ml of ethanol and chromium (III) nitrate nonahydrate (1 mmol) was heated in 10 ml of ethanol separately in the reaction vessel. A little triethylamine (TEA) was added to the container containing the ligand. Both substances were heated until they dissolved, and after the substances dissolved, the chromium(III) nitrate nonahydrate solution was added dropwise to the reaction vessel containing the ligand solution and mixed. The

reaction was refluxed for 3 hours. At the end of the period, the reaction was controlled by thin layer chromatography (10:1 ratio of DKM and MeOH). The material was filtered and washed with ethanol. For purification, the product was dissolved in methanol and allowed to crystallize. The obtained product was characterized by IR and LC/QTOF-MS spectral methods. IR-ATR and LC/QTOF-MS spectrumwererepresented in Supporting Information Fig. S5 and S6, respectively.

$[CrL_2]^+$ Complex: Henna green solid. Yield 60%. Degradation Point: 345-348°C. IR (ATR): 3435, 3277, 3044, 2971, 1644, 1595, 1566, 1537, 1438, 1381, 1325, 1300, 1153, 1131, 1044, 854, 800, 758, 653, 626, 558, 519, 465, 431 cm^{-1}; LC/QTOF-MS: *m/z* $[M-2H]^{2-}$ $(C_{18}H_{18}CrN_6O_2S_2)^{2-}$: Calcd: 466.0349. Obsd: 466.0339.

Synthesis of Fe(II) Complex

The synthesized carbotioamide compound (2 mmol) was heated in 20 ml of ethanol and iron (II) chloride tetrahydrate (1 mmol) in 10 ml of ethanol, separately in the reaction vessel. A little triethylamine (TEA) was added to the container containing the ligand. Both substances were heated until they dissolved, and after the substances dissolved, the iron (II) chloride tetrahydrate solution was added dropwise to the reaction vessel containing the ligand solution and mixed. After this process was completed, the substance was allowed to reflux again and was refluxed for 3 hours. At the end of the period, the reaction was controlled by thin layer chromatography (10:1 ratio of DKM and MeOH). The material was filtered and washed with ethanol. For purification, the product was dissolved in methanol and allowed to crystallize. The obtained product was characterized by IR analysis. IR spectrum was given in Supporting Information Fig. S7.

$[FeL_2]$ Complex: Black solid. Yield 58%. Degradation Point: 371-373°C. IR (ATR): 3453, 3322, 3168, 3074, 2914, 1593, 1534, 1492, 1471, 1435, 1361, 1306, 1282, 1232, 1158, 1128, 1079, 1047, 1013, 975, 941, 890, 847, 787, 753, 705, 643, 614, 578, 517, 426 cm^{-1}.

X-ray crystallography

The structure of HL compound was solved by direct methods and refined on F2 using all reflections[9]. Structural details and refinement data were given in Supplemental Table S1. Crystallographic data for the structural analysis were deposited at the Cambridge Crystallographic Data Center under accession number CCDC 2296872. The structure of the crystal was solved with the help of the OLEX2 program[10].

Hirshfeld Surface Analysis

Hirshfeld surface analysis and two-dimensional images of the molecule for which single crystal XRD analysis was performed were obtained with the Crystal Explorer21 (v.21.5) program[11]. Hirshfeld surface analysis of 2-(1-(2-hydroxyphenyl)ethylidene)-hydrazine-1-carbotioamide was viewed *via* normalized contact distance (dnorm) in line with the equation given in Eq. (1).

$$d_{norm} = \frac{d_i - r_i^{vdW}}{r_i^{vdW}} + \frac{d_e - r_e^{vdW}}{r_e^{vdW}} \quad \ldots (1)$$

d_i defines the distance between the Hirshfeld surface and the nearest nucleus inside the surface, and d_e defines the distance between the Hirshfeld surface and the nearest nucleus outside the surface. r^{vdW} represents the van der Waals radius of the relevant atom.

Computational Approach

The carbotioamide molecule and metal complexes were drawn in the GaussView 6.0 program [12]. The drawn structures were firstly performed with a preliminary optimization calculation using the universal force field (UFF) method[13]. In the result file obtained as a result of the calculation, the input file was re-created and all tautomer and conformer structures of the examined carbotioamide molecule were determined with the help of the Maestro 13.7 program, and the optimization calculation of each structure was performed again at the B3LYP-D3/6-31+G(d) level [14, 15]. All calculations were performed in the water phase and the conductive-like-polarized continuum model (C-PCM) method was used as the solvent method. When it came to the optimization calculation of metal complexes, all structures and bonding forms that could form complexes were taken into consideration and calculations were carried out. B3LYP-D3/6-31+G(d)(LANL2DZ) was also used in these optimization calculations [14,16].

Cell Viability Assays

The cytotoxic effects of the compounds in question were determined by performing the XTT test. Effect

of increasing concentrations of new compounds on cell viability for 24 and 48 hours by XTT (2,3-bis (2-methoxy-4-nitro-5-sulfophenyl)-5-[(phenylamino) carbonyl]-2H-tetrazolium hydroxide) test was investigated. The method is based on the principle that metabolically active cells reduce XTT, a tetrazolium salt, to orange formazan components.

Although the resulting dye is water-soluble, the dye density can be read at given wavelengths with the help of a spectrophotometer. Dye intensity (orange color) is proportional to the number of metabolically active cells. For cytotoxicity, first the relevant cancer cells were taken, 10×10^3 cells in each well, and planted in a sterile 96-well micro plate. Increasing concentrations of the synthesized compounds were applied to the cells and incubation was carried out for 24 and 48 hours. At the end of the incubation period, 50 µL of XTT solution was added to each well and incubated in a CO_2 oven for 4 hours. Then, the optical density (OD) value was read at 450 nm in the microplate reader. The cell viability rate of the control group was accepted as 100%, and cell viability was calculated with the help of Eq. (2):

$$\%\ Cell\ Viability = \frac{Concentration\ OD}{Control\ OD}\ x\ 100 \qquad \ldots (2)$$

Results and Discussion

Structure of 2-(1-(2-hydroxyphenyl)ethylidene)hydrazine-1-carbotioamide (HL)

2-(1-(2-hydroxyphenyl)ethylidene)hydrazine-1-carbotioamide (HL) molecule is synthesized according to the method mentioned in Section 2.3.1 and is characterized by spectral methods. In particular, single crystal XRD analysis of this molecule is also performed. The ORTEP diagram of the synthesized molecule is shown in Fig. 3.

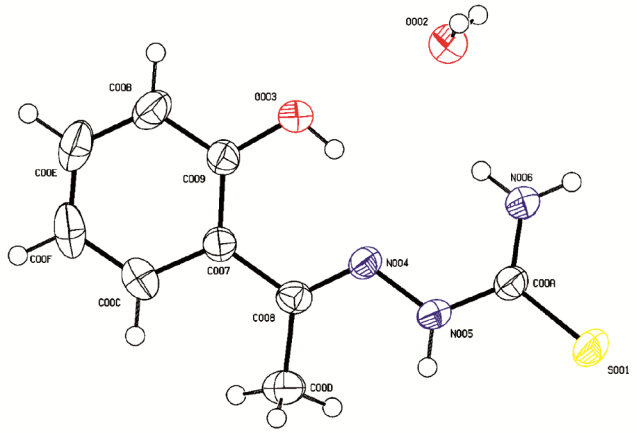

Fig. 3 — Molecular structure of HL compound

Tautomeric and conformer structures of the synthesized molecule are investigated with the Maestro 13.7 program. Each of the obtained isomeric structures is redrawn with the GaussView 6.0 program and optimized at the B3LYP-D3/6-31+G(d) level. After the calculation, no imaginary frequency is observed in the vibration frequencies obtained and it was decided that the structures obtained are stable structures. While the isomers of the molecule in question are shown in Fig. 4, the thermodynamic data of these structures are given in Table 1. These thermodynamic parameters in question are total energy (ET), enthalpy (H), Gibbs free energy (G) and entropy (S).

According to Table 1, it can be seen that the most stable isomeric structure is Iso1, and that Iso1 has the smallest value in other thermodynamic data except

Table 1 — Thermodynamic parameters of calculated isomer structures

Assignment	E_T[a]	H[a]	G[a]	S[b]
Iso1	–987.068	–987.067	–987.124	119.506
Iso2	–987.051	–987.050	–987.106	118.632
Iso3	–987.051	–987.050	–987.107	119.254
Iso4	–987.045	–987.044	–987.101	120.197
Iso5	–987.042	–987.041	–987.097	119.034
Iso6	–987.038	–987.037	–987.095	120.984

[a] in Hartree
[b] in cal/mol.K

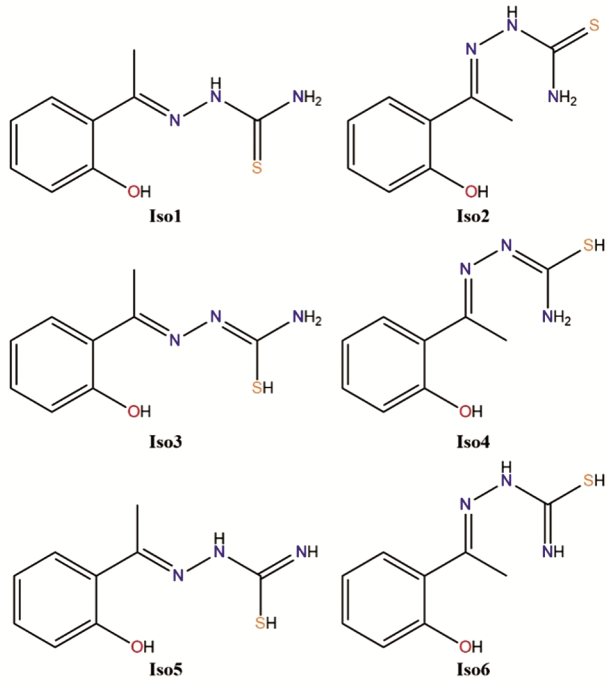

Fig. 4 — Calculated isomer structures of the synthesized carbonthioamide molecule

Table 2 — Structural parameters of the synthesized HL compound

Assignment	Experimental	Calculated
	Bond Length (Å)	
C00B-C009	1.386(3)	1.399
C009-O003	1.355(2)	1.374
C007-C008	1.478(3)	1.485
C008-C00D	1.493(3)	1.51
C008-N004	1.291(3)	1.294
N004-N005	1.387(2)	1.378
C00A-N005	1.344(3)	1.298
C00A-N006	1.315(3)	1.374
C00A-S001	1.693(2)	1.787
	Bond Angle (º)	
C007-C009-C00B	120.95(19)	120.77
C007-C008-C00D	118.84(18)	120.72
C007-C008-N004	117.68(17)	115.57
C008-N004-N005	117.27(16)	116.13
C00B-C009-O003	116.36(19)	121.33
N004-N005-C00A	121.30(16)	114.58
N005-C00A-N006	119.24(18)	118.94
N005-C00A-S001	119.14(15)	126.22
	Torsion Angle (º)	
O003-C009-C007-C008	–1.4(3)	2.1
C00C-C007-C008-N004	–174.9(2)	38.4
C00C-C007-C008-C00D	5.6(3)	138.71
C00D-C008-N004-N005	–5.3(3)	0.1
N004-N005-C00A-N006	–12.6(3)	–175.2
N004-N005-C00A-S001	168.15(15)	2.1

entropy, that is, the most stable structure. The geometric parameters of this isomeric structure and the experimentally obtained parameters are given in Table 2.

The results are subjected to regression analysis to determine the relationship between experimental and computational results more clearly. After the analysis, the regression coefficient obtained was found to be 0.9978. This value is very close to one and shows that there is a very good agreement between the experimental and computational results. Looking at the experimentally obtained ORTEP diagram, it was determined that there was a hydrogen bond between the hydrogen attached to the O003 atom and the N004 atom. The length of this hydrogen bond is measured as 1.899Å. The length of the hydrogen bond in Iso1, which is optimized at the B3LYP-D3/6-31+G(d) level, is calculated as 1.895 Å.

Complex Structures

The synthesized carbotioamide compound is reacted with chromium and iron metals and their salts. Since crystals could not be obtained from the complex compounds as a result of the reaction, their structures could not be elucidated experimentally. Possible structures of the synthesized complexes are

Table 3 — Thermodynamic parameters about possible complex structures

Assignment	E_T[a]	H[a]	G[a]
	Cr(III) Complex		
Structure 1 (Y1)	–2059.1735	–2059.1726	–2059.2602
Structure 2 (Y2)	–2059.1969	–2059.1959	–2059.2839
Structure 3 (Y3)	–2059.1009	–2059.1000	–2059.1980
Structure 4 (Y4)	–2059.1965	–2059.1955	–2059.2839
Structure 5 (Y5)	–2059.1746	–2059.1737	–2059.2626
	Fe(II) Complex		
Structure 1 (Y1)	–2096.2978	–2096.2968	–2096.3835
Structure 2 (Y2)	–2096.3524	–2096.3515	–2096.4382
Structure 3 (Y3)	ND[b]	ND[b]	ND[b]
Structure 4 (Y4)	–2096.2995	–2096.2985	–2096.3897
Structure 5 (Y5)	–2096.2933	–2096.2924	–2096.3818

[a] in Hartree
[b] No data

octahedral, square plane and distorted tetrahedral structures. These structures are drawn with computational chemistry programs and optimized at the B3LYP-D3/6-31+G(d)(LANL2DZ) level. Possible complex structures drawn in the GaussView 6.0 program are shown in Supporting Information Fig. S8. Thermodynamic parameters of Fe(II) and Cr(III) complexes are given in Table 3.

According to the thermodynamic data given in Table 3, it is seen that Y2 is the most stable structure in both iron and chromium complexes. It is observed that the atoms labeled S001, O003 and N004 of the ligand are connected to the metal atom by coordinated covalent bonds. The most stable structures of the complexes are shown in Fig. 5. Additionally, some structural parameters of these compounds are given in Supporting Information Table S2.

Similar metal (M) complexes synthesized and computationally analyzed in this study are discovered by Jezowska-Trzebiatowska *et al.*, in 1988 (Jezowska-Trzebiatowska *et al.*, 1988), by Orysyk *et al.*, in 2013 (Orysyk *et al.*, 2014), and by Sani and Yahaya in 2016 (Sani & Yahaya, 2016) and synthesized by Al-Hazmi and colleagues in 2021 (Al-Hazmi *et al.*, 2021). All of these studies are experimental, and in some of them, single crystal XRD analysis has been performed and structural parameters were revealed. According to these literatures, the bond length between M–O has been reported in the range of 1.855 – 2.037 Å (Orysyk *et al.*, 2014). In this study, the bond length between M–O was found to be in the range of 1.893 – 1.914 Å, and the results obtained appear to be in agreement with literature data. The bond length between M–N has been reported in the range of 1.884

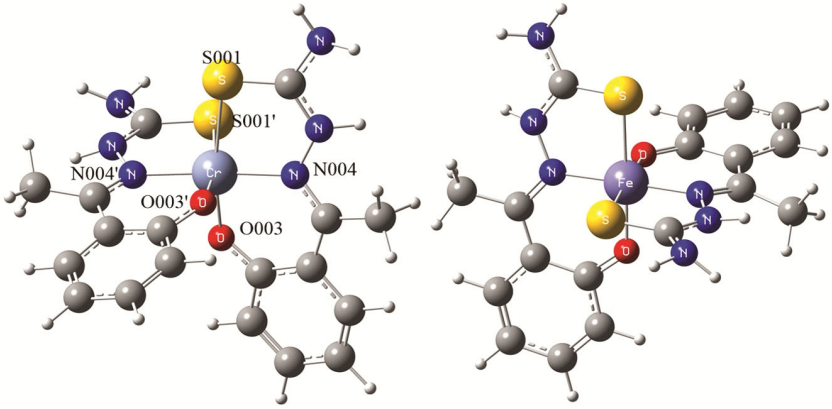

Fig. 5 — The most stable complex structures optimized at the B3LYP-D3/6-31+G(d) (LANL2DZ) level

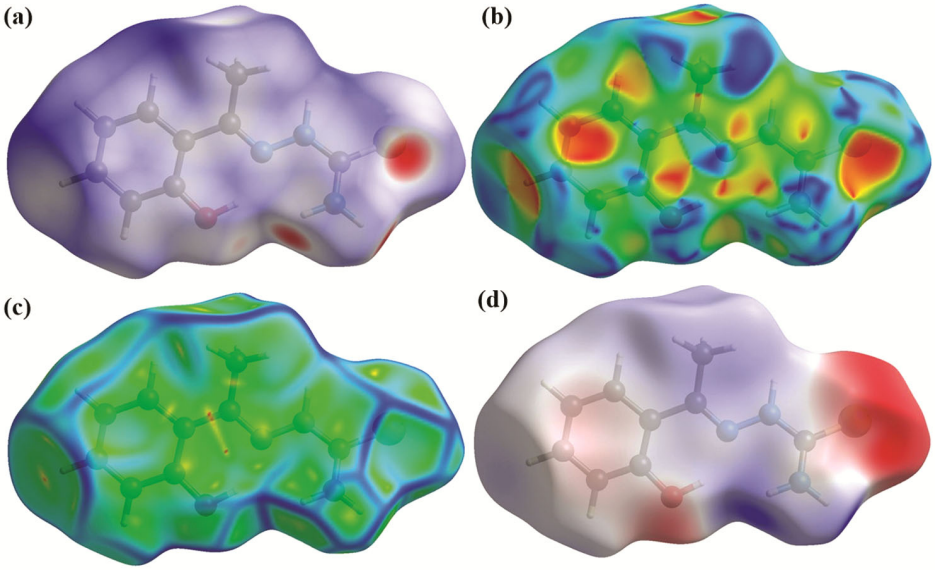

Fig. 6 — d_{norm} graph of the HL molecule (a) [color scale: –0.4100 (red) – 1.6010 (blue)], shape-index graph (b) [color scale: –1.0 (red) – 1.0 (blue)], curvature graph (c) [color scale: –4.000 (red) – 0.4000 (blue)] and electrostatic map (d) [color scale: –0.0665 (red) – 0.1254 (blue)].

– 2.135 Å (Orysyk *et al.*, 2014). In this study, the bond length between M–N was found to be in the range of 1.966 - 2.048 Å. The bond length between M–S was reported in the range of 2.148 - 2.490 Å by Orysyk and colleagues in 2014 (Orysyk *et al.*, 2014). In this study, the bond length between M-S was found to be in the range of 2.403 - 2.541 Å, and the results obtained are in agreement with literature data.

Hirshfeld Surface Analysis and Molecular Electrostatic Potential (MEP) Map

Hirshfeld surface analysis module for 2-(1-(2-hydroxyphenyl)ethylidene)hydrazine-1-carbotioamide molecule and some parameters such as volume (V), area (A), sphericity (G) and asphericity (Asp) are given in Table 4.

Table 4 — Properties of the obtained Hirshfeld surface analysis

V (Å^3)	A (Å^2)	G	Asp
243.86	244.58	0.772	0.279

The d_{norm} diagram, shape-index map, curvature graph and electrostatic map of the crystal of the relevant crystal molecule are shown in Fig. 6a – 6d, respectively. The resulting d_{norm} diagram reveals the interaction/contact map between molecules in the crystal. Depending on the interaction distance, red, white and blue colors appear on the surface of the molecule. While red implies that the interaction distance of the interacting atom is quite close, blue color implies that this distance is greater. Red, green and blue colors are observed in the shape-index map. The shape index map provides information about the

molecule surface. The regions dominated by red color represent the pit, while the blue color represents the protrusion on the surface of the molecule. The curvature map is used to reveal the flatness of the molecular surface and to determine aromatic interactions. In the curvature map calculated for the molecule, regions where π-π interaction may occur are shown in green. Finally, the electrostatic map of the molecule was calculated and the electron-rich and poor atoms in the molecule were determined.

When we look at the d_{norm} graph shown in Fig. 6a, there are red areas especially on the nitrogen and sulfur atoms. The presence of red regions especially around the hydrogen bonded to the nitrogen atom is due to the fact that these atoms can be used to make hydrogen bonds. According to the curvature graph of the synthesized carbotioamide compound, the corners are shown in blue, while the pits are represented in red. The green regions indicate planar regions. The curvature plot is very effective in defining the π-π interaction regions of the crystal. The presence of green regions indicates the most likely regions where π-π interaction can occur. Finally, the electrostatic map of the crystal was also obtained. The electrostatic map represents the electron density on the molecular surface, and electrons appear to be quite dense around the hetero atom. Additionally, the presence of slight redness on the benzene ring determined that the π electrons located in these parts were prone to interaction. The molecular electrostatic potential (MEP) maps of this molecule in question were also calculated using computational chemistry methods and are shown in Supporting Information Fig. S9.

According to Fig. S9, it appears that red colors are dominant around the oxygen atoms in the molecule, followed by yellow. This means that electrons are concentrated in these regions and that these parts are suitable for electrophilic attack. It was also determined that the yellow colors on the benzene rings in the molecule were due to the delocalization of π electrons in this region. The interaction fingerprint map of the resulting crystal was obtained and shown in Fig. 7a.

According to the interaction fingerprint map in the crystal shown in Fig. 7, the interaction map in which the oxygen atom in the relevant molecule is bonded with the hydrogen atom in the other molecule is shown in Fig. 7b and corresponds to 4.2% of the total interaction. The map of the interaction of sulfur and nitrogen atoms, which are hetero atoms in our molecule, with hydrogen atoms in the other molecule, is shown in Fig. 7c and 7d, respectively, and corresponds to 14.1% and 1.7% of the total interaction. Fig. 7e shows the interaction map of the hydrogen atom on the nitrogen atom with the oxygen atom on the neighboring molecule, and it was found that 5.6% of the total interaction resulted from this interaction. In general, it is observed that the hydrogen-hydrogen interaction is dominant.

Spectral Analysis

IR Spectra

IR spectra of the synthesized ligand and complexes are obtained experimentally and used to characterize the molecules spectrally. In addition to the experimentally obtained spectrum, IR spectra are also obtained computationally for all molecules. Labeling is carried out by comparing observed strain frequencies with experimental frequencies. Finally, the vibration frequencies between the complexes and the ligand were also compared. The IR spectrum of the compound 2-(1-(2-hydroxyphenyl)ethylidene) hydrazine-1-carbotioamide calculated at the B3LYP-D3/6-31+G(d) level is shown in Fig. 8.

The peaks in the IR spectrum shown in Fig. 8 are labeled and compared with the experimental results. The vibration frequencies calculated for the synthesized molecule are given in Table 5.

The computational results given in Table 5 are anharmonic frequencies. The frequencies given experimentally are known as harmonic frequencies. Computationally, values known as scale factors[21] are used to convert anharmonic frequencies into harmonic frequencies. However, there is no scale factor for each calculation level, and since there is no scale factor for the calculation level we use, the frequencies are given anharmonic. As seen in Table 5, anharmonic frequencies generally have higher values than harmonic frequencies. Vibrational frequencies of similar molecules of the synthesized molecule have been reported. It is determined that the vibration frequency of each labeled bond is in compliance with the literature given in Table 5. Additionally, the regression coefficient for agreement between computational and experimental values is calculated as 0.994. This result shows that the obtained results are in harmony with each other.

The IR spectra of the complexes are calculated at the B3LYP-D3/6-31+G(d)(LANL2DZ) level and are shown in Supporting Information Fig. S10. In addition, the vibration frequencies, labeling and

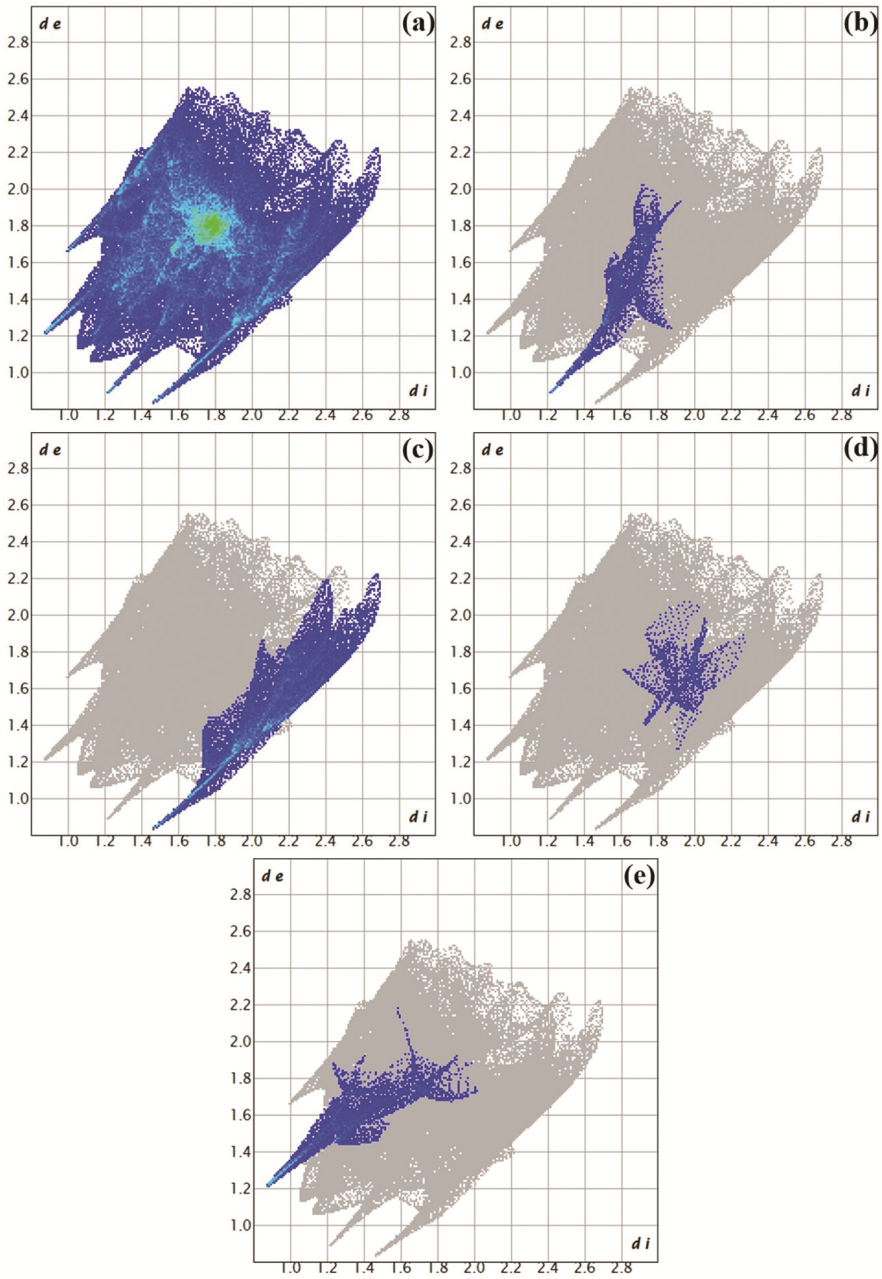

Fig. 7 — Finger print map of the interaction of the obtained crystal

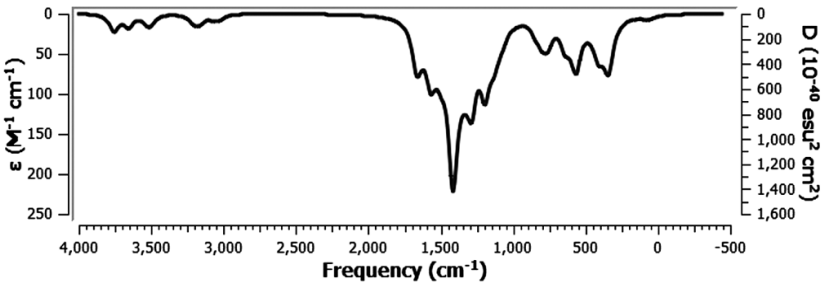

Fig. 8 — Simulated IR spectrum of HL

Table 5 — Experimental and calculated stretching frequencies (cm^{-1}) of selected functional group of HL

Assignment	Calculated	Experimental	References
ν_{OH}	3757	3405	17
ν_{NH}	3656, 3524	3286	17
$\nu_{CH\ Aromatik}$	3206	3139	18
$\nu_{CH\ Alifatik}$	3024	2954	19
$\nu_{C=N}$	1652	1589	17
ν_{C-N}	1288	1278	18
ν_{C-O}	1272	1237	19
ν_{N-N}	1191	1165	20
$\nu_{C=S}$	804	821	17

comparison of the peaks observed in the spectra with the experimental vibration frequencies are given in Table S3.

According to Table S3, significant differences are observed depending on the frequency values of the ligand. First of all, due to the increase in the number of NH bonds in complex compounds, experimentally the bond tension frequency increased up to 3400 cm^{-1}. This situation is observed in the same way computationally. The C=S bond is observed both in complexes and in complexes around 820 cm^{-1}. Finally, the bond voltage frequencies between the metal atom and the donor atom are observed experimentally and computationally. These frequencies are not in the IR spectrum of the ligand, but are observed in the IR spectrum of the complex. This shows that there is complexation in this case. Finally, the voltage frequency of the bond between metal and sulfur could not be determined in the experimental spectrum because it was outside the observation range. However, it was observed that the frequency determined computationally was in line with the data in the article published by Schelvis *et al.* in 2002[22]. As a result, it is determined that the obtained vibration frequencies of both the ligand and the complexes are in harmony with each other, support each other, and can be shown as evidence that the complexation reaction has been carried out correctly and complex compounds have been obtained.

NMR Spectra

NMR spectra of HL are obtained both experimentally and computationally. Experimentally, ^{1}H-NMR and ^{13}C-NMR spectra are taken in DMSO-D6 solvent. While the proton in the hydroxyl (OH) in the synthesized carbotioamide compound is observed as a singlet at 12.69 ppm, the same proton is calculated at 12.15 ppm. While the protons in the $–CSNH_2$ group are observed as singlets at 10.58 ppm, the chemical shift values of these protons are calculated as 9.56 ppm. Likewise, the proton in the –NHCS– group is observed experimentally at 8.10 ppm, while it is observed computationally at 8.37 ppm. While the protons in the benzene ring are observed at 7.47 - 6.81 ppm, the chemical shift values of these protons are calculated in the range of 7.69 - 6.91 ppm.

When looking at the ^{13}C-NMR spectrum, the chemical shift value of the carbon atom in the C=S group is observed as 181.17 ppm, while this value is calculated as 173.19 ppm. In addition, the chemical shift value of the carbon atom to which the hydroxyl group in the benzene ring is attached is observed as 157.79 ppm. Computationally, the chemical shift value of the relevant carbon atom is calculated as 148.63 ppm. While the chemical shift value of the carbon atom in the imine group is observed as 153.66 ppm, it is calculated as 141.01 ppm. While the chemical shift value of the methyl group is observed as 24.67 ppm, it is calculated as 25.13 ppm. Finally, the chemical shift values of the carbon atoms in the benzene ring are observed in the range of 131.11 - 116.88 ppm, while the chemical shift values of these carbon atoms are calculated as 125.95 - 109.94 ppm.

Mass Spectra

The synthesized 2-(1-(2-hydroxyphenyl)ethylidene) hydrazine-1-carbotioamide compound is subjected to liquid chromatography-time-of-flight mass spectrometry (LC/QTOF-MS) analysis. The closed formula of this synthesized compound is $C_9H_{11}N_3OS$ and the expected mass/charge (m/z) ratio of the anion that has lost a proton was calculated as 208.055. The experimentally obtained chromatogram and spectrum are represented in Fig. S4. According to this chromatogram, only one peak is observed, indicating that the crystal obtained is highly pure. In the spectrum, a peak with an m/z ratio of 208.0552 was observed, and due to the isotope atoms in the relevant molecule, the m/z ratio was observed as 209.0582, 211.0546, and 212.0555. The agreement score between the calculated m/z ratio and the observed m/z ratio was calculated as 98.82.

LC/QTOF-MS analysis is performed on the synthesized $[FeL_2]$ and $[CrL_2]$+ complexes. For the $[FeL_2]^-$complex, the m/z ratio could not be determined because the molecule was fragmented. When looking at the chromatogram of this molecule, the mass of the ligand is observed to be dominant. When it comes to the $[CrL_2]$+ complex, the LC/QTOF-MS spectrum is shown in Supp. Fig. S6.

Table 6 — Cell viability percentages on the mentioned cancer cells at different concentrations

Compound	100 μM	50 μM	25 μM	10 μM	1 μM	0.1 μM	IC_{50} (μM)
Breast Cancer (MCF-7, ATCC Code: HTB-22)							
HL	42.07	44.88	36.41	49.12	51.71	52.32	**11.01**
$[FeL_2]$	58.13	56.26	53.77	55.52	67.91	69.17	**1.62**
$[CrL_2]^+$	43.65	43.66	48.64	70.78	71.40	69.54	**21.80**
Colon Cancer (HT-29, ATCC Code: HTB:38)							
HL	86.22	84.47	78.6	80.87	82.76	85.22	-
$[FeL_2]$	80.22	80.76	76.99	77.72	86.88	92.52	-
$[CrL_2]^+$	71.14	90.59	82.17	78.92	92.43	83.58	-
Gastric Cancer (SNU-16, ATCC Code: CRL-5974)							
HL	70.70	87.93	89.89	104.87	109.53	88.30	-
$[FeL_2]$	68.97	86.34	85.75	91.96	122.46	88.58	-
$[CrL_2]^+$	74.05	67.07	66.26	85.29	105.23	77.77	-

The experimentally found m/z ratio for this molecule is 466.0339. However, the $(M-H)^-$ m/z ratio of the state of the same molecule that has lost a proton, that is, the theoretical ratio, was determined as 469.0578 with the MestReNova program (Version: 12.0.0-20080). The apparent mass is thought to be the m/z ratio of the $(M-4H)^{4-}$ ion instead of $(M-H)^-$. Considering the studies conducted by Griffeycor *et al.* in 1997 and Zamfir *et al.* in 2011, it was proven that the m/z ratios of the $(M-4H)^{4-}$ ion has been determined by LC/QTOF-MS analysis[23]. It is decided that the experimentally obtained result is similar to the results in the literature and belonged to the $(M-4H)^{4-}$ ion of the $[CrL_2]^+$ complex.

Cell Viability Assay

Cell viability analysis of the synthesized HL, $[FeL_2]$ and $[CrL_2]^+$ labeled compounds on breast (MCF-7), colon (HT-29) and stomach cancer (SNU-16) cell lines is performed using the XTT method. Initially, stock solutions of these molecules at 1mM concentration are prepared. The effectiveness of the molecules synthesized against the mentioned cancer cell lines is investigated in different concentrations (100 μM, 50 μM, 25 μM, 10 μM, 1 μM and 0.1 μM) and in 3 replicate studies. The cell viability percentage is determined by the XTT colorimetric method 24 hours after the application and the obtained cell viability percentages are given in Table 6. The obtained data are uploaded to the AAT Bioquest web tool and IC_{50} values are calculated. IC_{50} values obtained against the mentioned cancer cells are given in Table 6.

According to Table 6, synthesized molecules are ineffective against colon and stomach cancer cell lines. However, they are also observed to be effective against breast cancer cell lines at low concentrations. The cell viability percentage of the Fe(II) complex at all concentrations is observed to be close to 50%. It is determined that the cells lost their viability through necrosis rather than the apoptosis pathway, and that the presence of the relevant compound rather than the concentration caused this situation. This compound is determined to have the lowest IC50 value. In addition, the IC50 value of the ligand and Cr(III) complex against the breast cancer cell line is determined as 11.01 and 21.80 μM, respectively.

Conclusions

Carbotioamide derivative and metal complexes were synthesized and characterized by IR, NMR, MS and single crystal XRD. Then, synthesized ligand molecule are optimized at B3LYP-D3/6-31+G(d) level and B3LYP-D3/6-31+G(d)(LANL2DZ)is used in the optimization of metal complexes.Hirshfeld surface analyses are investigated for obtained crystal. Electronic properties of Schiff bases are investigated based on molecular electrostatic potential map. The anticancer properties of all molecules are investigated by *in vitro* methods. Cell viability assays is performed using XTT tests. Three different cancer cell lines were used in this analysis. MCF-7 for breast cancer; HT-29 cell lines were used for colon cancer and SNU-16 cell lines for gastric cancer. It was found that synthesized compounds are only active against breast cell line, MCF-7. The best compound was found as $[FeL_2]$ due to the fact that its IC_{50} was calculated as 1.62 μM.

Supplementary Information

Supplementary information is available in the website http://nopr.niscpr.res.in/handle/123456789/58776.

Acknowledgements

The numerical calculations reported in this paper were fully/partially performed at TUBITAK ULAKBIM, High Performance and Grid Computing

Center (TRUBA resources). This work was supported by the Scientific Research Project Fund of Sivas Cumhuriyet University (CUBAP) under the project number F-2022-672.

References

1 Lobana T S, Sultana R, Hundal G & Butcher R J, *Dalton Trans*, 39 (2010) 7870.

2 Wang F, Langley R, Gulten G, Dover L G, Besra G S, Jacobs W R & Sacchettini J C, *J Exp Med*, 204 (2007) 73.

3 Tahlan S, Narasimhan B, Lim S M, Ramasamy K, Mani V & Shah S A, *Mini Reviews Med Chem*, 19 (2019) 1080.

4 Cicekbilek F, Yilmaz B, Bayrakci M & Gezici O, *J Fluorescence*, 29 (2019) 1349.

5 Bayrakcı M, Özcan F, Yılmaz B & Ertül Ş, *Acta Chim Slov*, 64 (2017) 679.

6 Vicini P, Geronikaki A, Incerti M, Busonera B, Poni G, Cabras C A & La Colla P, *BioorgMed Chem*, 11 (2003) 4785.

7 Al-Hazmi G, El-Metwally N, El-Gammal O & El-Asmy A, *Spectrochim Acta Part A: Mol Biomol Spect*, 69 (2008) 56.

8 Sheldrick, G. SHELXTL V5. 1, Software Reference Manual, Bruker AXS, Inc., Madison, Wisconsin, USA, 1997. *Received May* 2000, 26, I00217.

9 Sheldrick G M, *Acta Crystallograph Sec A: Found Crystallograp*, 64 (2008) 112.

10 Dolomanov O V, Bourhis L J, Gildea R J, Howard J A & Puschmann H, *J App Crystallograp*, 42 (2009) 339.

11 Spackman P R, Turner M J, McKinnon J J, Wolff S K, Grimwood D J, Jayatilaka D & Spackman M A, *J App Crystallograp*,, 54 (2021) 1006.

12 *Gauss View, Version 6.1*; Semichem Inc. Shawnee Mission, KS, 2016.

13 Rappé A K, Casewit C J, Colwell K, Goddard III W A & Skiff W M U F F, *J Am Chem Soc*, 114 (1992) 10024.

14 (a). Becke A D, *J Chem Phys,* 96 (1992) 2155; (b). Ditchfield R, Hehre W J & Pople J A, *J Chem Phys*, 54 (1971) 724; (c). Hariharan P C & Pople J A, *Theoretica Chimica Acta*,, 28 (1973) 213; (d) Hehre W J, Ditchfield R & Pople J A, *J Chem Phys*, 56 (1972) 2257; (e). Rassolov V A, Pople J A, Ratner M A & Windus T L, *J Chem Phys*, 109 (1998) 1223; (f) Rassolov V A, Ratner M A, Pople J A, Redfern P C & Curtiss L A, *J Comp Chem*,, 22 (2001) 976.

15 (a).Binning R & Curtiss L, *J Comp Chem*, 11 (1990) 1206; (b) Blaudeau J-P, McGrath M P, Curtiss L A & Radom L, *J Chem Phys*, 107 (1997) 5016; (c) Francl M M, Pietro W J, Hehre W J, Binkley J S, Gordon M S, DeFrees D J, Pople J A, *J Chem Phys,* , 77 (1982) 3654; (d) Gordon M S, *Chem Phys Lett*,76 (1980) 163; (e) Hariharan P & Pople J A, *Mole Phys,* , 27 (1974) 209; (f) Petersson A, Bennett A, Tensfeldt T G, Al-Laham M A, Shirley W A, Mantzaris J, *J Chem Phys*, 89 (1988) 2193; (g) Petersson G, Al-Laham M A, *J chemical Phys*, 94 (1991) 6081.

16 (a) Dunning T H, Hay P J & Schaefer H, *Mode Theore Chem*, 3 (1977) 1; (b) Hay P J & Wadt W R, *J Chem Phys*, 82 (1985) 270; (c) Wadt W R & Hay P J, *J Chem Phys*,82 (1985) 284.

17 Sani U & Yahaya M, *Chem Search J*, 7 (2016) 57.

18 Ahsan M J, Samy J G, Soni S, Jain N, Kumar L, Sharma L K, Yadav H, Saini L, Kalyansing R G & Devenda N S, *Bioorg Med Chem Lett*,, 21 (2011) 5259.

19 Orysyk S, Repich G, Bon V, Dyakonenko V, Orysyk V, Zborovskii Y L, Shishkin O, Pekhnyo V & Vovk M, *Inorg Chim Acta,* , 423 (2014) 496.

20 Orysyk S, Bon V, Zholob O, Pekhnyo V, Orysyk V, Zborovskii Y L & Vovk M, *Polyhedron*, 51 (2013) 211.

21 Ünal Y, Nassif W, Özaydin B C & Sayin K, *Vibrational Spectroscopy*,, 112 (2021) 103189.

22 Schelvis J P, Berka V, Babcock G T & Tsai A-l, *Biochem*, 41 (2002) 5695.

23 (a) Griffeycor R H, Sasmor H & Greig M J, *J Am Soc Mass Spectromet*, 8 (1997) 155; (b) Zamfir A D, Flangea C, Sisu E, Seidler D G & Peter-Katalinić J, *Electrophoresis*, 32 (2011) 1639.